Solid Earth Discuss., 6, 1765–1798, 2014
www.solid-earth-discuss.net/6/1765/2014/
doi:10.5194/sed-6-1765-2014

Solid Earth
Discussions
Open Access

Recognition of a porphyry system using ASTER data in Bideghan – Qom province (central of Iran)

F. Feizi[1] **and E. Mansouri**[2]

[1]Department of Mining Engineering, South Tehran Branch, Islamic Azad University, Tehran, Iran
[2]Young Researchers and Elite Club, South Tehran Branch, Islamic Azad University, Tehran, Iran

Received: 2 July 2014 – Accepted: 3 July 2014 – Published: 18 July 2014

Correspondence to: F. Feizi (feizi.faranak@yahoo.com)

Published by Copernicus Publications on behalf of the European Geosciences Union.

Abstract

The Bideghan area is located south of the Qom province (central of Iran). The most impressive geological features in the studied area are the Eocene sequences which are intruded by volcanic rocks with basic compositions. Advanced Space borne Thermal Emission and Reflection Radiometer (ASTER) image processing have been used for hydrothermal alteration mapping and lineaments identification in the investigated area. In this research false color composite, band ratio, Principal Component Analysis (PCA), Least Square Fit (LS-Fit) and Spectral Angel Mapping (SAM) techniques were applied on ASTER data and argillic, phyllic, Iron oxide and propylitic alteration zones were separated. Lineaments were identified by aid of false color composite, high pass filters and hill-shade DEM techniques. The results of this study demonstrate the usefulness of remote sensing method and ASTER multi-spectral data for alteration and lineament mapping. Finally, the results were confirmed by field investigation.

1 Introduction

Iran is located in the Alpine–Himalayan orogenic belt and Uromieh–Dokhtar metalogenic belt is the most impotant zone in Iran which has high potentials for gold and copper as well as other base metal deposits. In Iran, satellite data such as TM, ETM+ and ASTER (Advanced Spaceborne Thermal Emission and Reflection Radiometer) have been used by geologists for exploration purposes (Asadi Haroni and Lavafan, 2007; Azizi et al., 2010).

Intermediate to acidic igneous rocks from the late Cretaceous to Tertiary in the western, northwestern and northern parts of Iran are important because the high value presence of copper and gold mineralization in these host rocks. These rocks have been found in the 1 : 100 000 Kahak sheet. The studied area is located in this geological map as a part of Uromieh–Dokhtar belt. Therefore, high resolution remote sensing data and Geographic Information Systems (GIS) are important tools to map subtle anomalies associated with unknown gold and base metal deposits (Kujjo, 2010; Bell, 2011; Albanese, 2011).

Because the alteration zones recognition are the most important keys for base metal deposit exploration therefore using of methods such as remote sensing which help to separate theses zones will be useful.

In this research, a spectral analysis was carried out on the ASTER satellite imagery data of the investigated area to map spectral signatures associated with the hydrothermal alterations. Least Square Fit (LS-Fit), Principal Components Analysis and band ratio methods were also performed to achieve better accuracy along with spectral analysis. In addition, lineaments by using of False Color Composite (FCC) images, high pass filters and hill-shade DEM techniques were extracted.

Finally the integration of alteration, lineaments and lithologiical features can show the hopeful areas for exploration.

2 Materials and methods

2.1 Geology setting

The studied area is located between 50°56′, 50°59′ longitude and 34°17′, 34°20′ latitude in the south of the Qom province (Northeast of 1 : 100 000 KAHAK Sheet). Based on 1 : 100 000 geological map of Qom, the most impressive lithological features in the studied area are the volcanic rocks with basic combinations. These features are included; Andesite, Andesibasalt and megaporphytite andesite. There are tuffaceous sandstone and limestones in the east and southeast of the investigated area. Hematitation, limonitation, silisitaion and argillic alterations are seen in central parts that have been formed in north-south trend in the east and northeast of the studied area. Volcanic rocks have specific conditions. For example, ferrous ore such as Oligist formed along fractures in a tectonic environment. (Agha Nabati, 2004). Based on 1 : 100 000 geological map of Kahak, three NE-SW faults have been seen. According to study results conducted around the faults, alteration and ferrous fluid have been observed (Fig. 1).

2.2 ASTER data

The ASTER is an advanced optical sensor comprised of 14 spectral channels ranging from the visible to thermal infrared region. It will provide scientific and also practical data regarding various field related studies of the earth (Watanabe and Matsuo, 2003). Various factors affect the signal measured at the sensor such as the drift of the sensor radiometric calibration, atmospheric and topographical effects. For accurate analysis, all of these corrections are necessary for remote sensing imagery. To this end, at the beginning of the path, data set in hierarchical data format (HDF) was used for this research and radiance correction such as wavelength, dark subtract and log residual by ENVI4.4 software which was essential for multispectral images were implemented. ASTER bands have good sensitivity for alteration minerals. For example VNIR band is good for Iron oxide and SWIR is good for argillic alteration in band 4, propellitic alteration in band 6 and phyllic alteration in band 4, 5 or 8 usually. Also TIR include thermal bands for silica identification usually.

3 Result and discussion

3.1 Hydrothermal alteration detection

Many image analysis and processing techniques can be used to interpret the remote sensing spectral data. In this research, False Color Composite (FCC), Minimum Noise Fraction (MNF), Principal Component Analysis (PCA), Least Square Fit (LS-Fit) and Spectral Angle Mapping (SAM) methods were used on the ASTER data for the discrimination of alteration zones.

SED
6, 1765–1798, 2014

3.1.1 False Color Composite (FCC)

The studies on re-sampling of USGS standard curves on ASTER bands show that Al-OH minerals such as kaolinite, muscovite, montmorilonite and illite (major minerals for phyllic and argillic alteration zones) have the most reflection in B4 on SWIR (Fig. 2). Also, Mg-OH minerals such as chlorite and epidote that are remarkable for propylitic alteration zones have the most reflection in Band 5 and 6 on SWIR (Yetkin et al., 2004, Fig. 3).

Therefore, phyllic and argillic alteration zones are shown reddish to pink and propylitic alteration zones are shown green in 468 False Color Composite (FCC) on SWIR (Beiranvnd Pour et al., 2011, Fig. 4).

3.1.2 Principal Component Analysis

The Principal Component Analysis (PCA) is a multivariate statistical technique that selects uncorrelated linear combinations (eigenvector loadings) of variables. Each successively extracted linear combination, or principal component (PC), has a smaller variance. The PCA is widely used for alteration mapping in metallogenic provinces (Myint et al., 2005) and has been applied in this study. An approach based on the examination of eigenvector loadings in each PC image is used for determining which image contains information related to the spectral signatures of specific target minerals. It is expected that the PC image that collects moderate to high eigenvector loadings for the diagnostic absorptive and reflective bands of the index mineral could be considered as the specific image for that mineral. If the loading of the absorptive band is negative in sign the target area will be enhanced in bright pixels, and if the loading of the reflective band is negative the area will be enhanced in dark pixels (Crosta and Moore, 1989; Khaleghi and Ranjbar, 2011).

Table 1 shows the eigenvector loadings for bands 1, 2, 3 and 4. In this Table at a $\frac{2}{1}$ ratio and at a $\frac{3}{1}$ ratio should not be + or – both. These ratios must be $\frac{+}{-}$ (normal case) or $\frac{-}{+}$ (inverse case). Inverse case has to correct. The analyses which have done on

SED
6, 1765–1798, 2014

Table 1 show in PC3, $\frac{3}{4}$ ratio is $\frac{-}{+}$ so it should study in inverse case. In PC4 $\frac{2}{1}$ ratio is $\frac{-}{+}$ and $\frac{3}{4}$ ratio is $\frac{+}{-}$ so PC4 have to study in both case. Base on this investigation PC3 shows good results in inverse case. Inverse of PC3 can show the areas with iron oxide. Table 2 shows the eigenvector loadings for bands 1, 4, 5 and 7. In PC1, $\frac{5}{7}$ ratio is $\frac{+}{-}$ so it should study in normal case. In PC2 $\frac{4}{1}$, $\frac{5}{7}$ ratios are $\frac{+}{-}$ so they should study in normal case. In PC3, $\frac{4}{1}$ ratio is $\frac{+}{-}$ so it should study in normal case. In PC4 $\frac{4}{1}$, $\frac{5}{7}$ ratios are $\frac{-}{+}$ so they should study in inverse case. Base on this investigation PC3 shows good results in normal case. According to the results, the image related to PC3 shows the argillic alteration. Table 3 shows the eigenvector loadings for bands 1, 3, 5 and 6. In PC2, $\frac{3}{1}$ ratio is $\frac{-}{+}$ so it should study in inverse case and In PC3, $\frac{3}{1}$ and $\frac{5}{6}$ ratios are $\frac{+}{-}$ so they should study in normal case. In PC4, $\frac{3}{1}$ ratio is $\frac{-}{+}$ so it should study in inverse case. Base on this investigation PC4 shows good results in inverse case. Inverse of PC4 can show the areas with phyllic alteration. Table 4 shows the eigenvector loadings for bands 2, 5, 8 and 9. In PC2, $\frac{5}{2}$ ratio is $\frac{+}{-}$ so it should study in normal case. In PC3, $\frac{5}{2}$, $\frac{8}{9}$ ratios are $\frac{+}{-}$ so they should study in normal case. In PC4, $\frac{5}{2}$ ratio is $\frac{+}{-}$ so it should study in normal case. Base on this investigation PC4 shows good results in normal case. PC4 can show the areas with propylitic alteration (Fig. 5).

3.1.3 Least Squares Fitting (LS-Fit)

The technique assumes that the bands used as input values are behaving as the variables of a linear expression and the "*y*" value of the equation, namely the predicted band information, gives us a calculated output value. This predicted band is what the band should be according to the linear equation. The minerals which are sensitive to a specific band are then differentiated from the features which are reflective to the other bands as well by simply taking the difference between the predicted values and the original values (Yetkin et al., 2004).

Distribution of iron oxide was created by using all three visible and near-infrared (VNIR) bands as the input bands and VNIR-b1 as the modeled band. Also, argillic, phyllic and propylitic alterations were mapped by using residual band SWIR-b1, residual band SWIR-b3 and residual SWIR-b6 (Fig. 6).

3.1.4 Minimum Noise Fraction (MNF)

The Minimum Noise Fraction (MNF) transformation was used to determine the inherent dimensionality of image data, segregate noise in the data and reduce the computational requirements for subsequent processing (Boardman et al., 1995; Green et al., 1988; Beiranvnd Pour et al., 2011). PCA is a method for decreasing repetitive data and nuisance features as shades,topographical effects and sun radiation angel. This method is based on standard deviation, variance and covariance calculations. MNF like PCA is good for decreasing later calculations. In his research, both methods were used for controlling the results with comparing them. MNF involves two steps. In the first step, which is also called noise whitening, principal components for noise covariance matrix are calculated. This step decorrelates and rescales the noise in the data. In the second step, principal components are derived from the noise whitened data. The data can then be divided into two parts. One part associated with large Eigen values and the other part with near unity Eigen values and noise dominated images. Using data with large Eigen values separates the noise from the data, and improves spectral results (Green et al., 1988; Beiranvnd Pour et al., 2011). MNF analysis can identify the locations of spectral signature anomalies. This process is of interest to exploration geologist because spectral anomalies are often indicative of alterations due to hydrothermal mineralization (Beiranvnd Pour et al., 2011). MNF bands 2, 6, 4 (inverse) and 5 were used for iron oxide, argillic, phyllic and propylitic alterations (Fig. 7).

3.1.5 Spectral Angle Mapper

The Spectral Angle Mapper (SAM) is a classification technique that permits rapid mapping by calculating the spectral similarity between the image spectrums and reference reflectance spectra. SAM measures the spectral similarity by calculating the angle be-

SED
6, 1765–1798, 2014

tween the two spectra and treating them as vectors in n-dimensional space (Kruse et al., 1993), (Beiranvnd et al., 2011). The image spectra were compared with USGS Digital Spectral Library (Minerals) (Malekzadeh et al., 2009). Figure 8 shows selected minerals spectral library plots that related to argillic, phyllic and propylitic alterations. Three mineral spectral representatives of the argillic zone include kaolinite, dickite and halloysite. Two minerals spectral representatives of the phyllic alteration consist of illite, muscovite, and epidote. Chlorite representative of propylitic zone were selected (Fig. 9).

4 Lineament extraction

Lineament extraction in this study was carried out by manual method. In manual extraction method, the lineaments are extracted from a satellite image by using visual interpretation. In this research Shaded relief method and median filter were used for fault identification with using DEM image which was prepared by Geological survey of Iran. The lineaments usually appear as straight lines or "edges" on the satellite images which in all cases were contributed to the tonal differences within the surface material. The knowledge and the experience of the user is the key point in the identification of the lineaments particularly to connect broken segments into a longer lineament (Sarp, 2005).

False color images are produced for manual lineament extraction because they increase the interpretability of the data. Different combinations of three bands are examined and the best visual quality is obtained with a false color image utilizing three 7, 4, and 2 (in blue, green and red respectively). This false color combination made it easier to identify linear patterns of vegetation, geologic formation boundaries, river channels and geological weakness zones. Moreover, filtering operations are used to emphasize or deemphasize spatial frequency in the image. The filtering operation will sharpen the boundary that exists between adjacent units. Furthermore, standard GIS techniques have been carried out to help in the evaluation of the lineaments detected.

SED
6, 1765–1798, 2014

Digital Elevation Model (DEM) has the advantage of representing the vertical extension of the earth's surface by assigning height values for every pixel (Papadaki et al., 2011). The Hill-shade DEM technique is also effective in creating images that enhance geomorphologic features (Weldemariam, 2009). Therefore, Hill-shades DEM with different azimuth direction and sun angle were used in this study (Fig. 10).

5 Integration of alteration and lineament

In this part for integration the data layers in GIS area, first of all, the shape files of all alteration zones which were carried out with different methods were drown. Then the layers were overlapped on each other. Afterwards the most overlapped zones were chosen and were controlled with field investigations. As the last step, the lineament map of studied area was integrated with the final alteration map in GIS area. (Fig. 11). As the figure shows, there is a very good adaptation between these two layers, especially in the east and a band with a NW–SE trend in the south of the area. There is also a good adaptation in north of the area. Therefore, a circular band that begins from the northwest corner to the east, southeast and to the west has been recognized.

6 Field investigations and alteration zones control

After all these software analyses, field investigations were necessary. Figure 12 shows a full view of studied area. The control points were detected, and after the field studies, the correction of alteration zones were confirmed. Figure 13 shows the three check points for Iron oxide which were recognized with using remote sensing processes. These checking have confirmed the results of the RS methods.

As Fig. 14 shows, Sericitic Muscovites, Quartz and a few of Illite have been seen in the Phllic alteration zones. The check field for Argillic alteration zones were confirmed by the results of RS methods (Fig. 15). Presence of Chlorite and Epidote minerals in

SED
6, 1765–1798, 2014

check field processes confirmed the Propylitic alteration zones (Fig. 16). The adaptation of Iron Oxide and Argillic alteration zones is a very important guide for hydrothermal mineralization deposits, especially sulfide minerals (Fig. 17).

7 Mapping hydrothermal alteration at porphyry copper deposits

Most of the world's copper is mined from porphyry deposits which occur in a different geologic environment. Hydrothermal alteration is also common at porphyry deposits and may be recognized by the same methods that were developed in remote sensing.

7.1 Alteration model

According to the model of hydrothermal alteration of porphyry copper deposits that was developed by Lowell and Guilbert (1970), Phyllic zone is the most intense alteration which occurs in the core of the porphyry body and contains Quartz, Sericite and Pyrite. Other alteration zones are Argillic and Propylitic. The most characteristic minerals in Argillic zone are Quartz, kaolinite and montmorillonite. Propylitic zone contains Epidote, calcite, and chlorite. The existence of these alterations is important key for exploration of this kind of deposits, especially, with remote sensing methods.

The ore body includes disseminated grains of Chalcopyrite, Molybdenite, Pyrite and other metal Sulfides. The most of this mineralization occurs near the boundary between the Potassic and Phyllic zones.

The porphyry copper deposits have a red to brown iron-stained crust called Gossan or leached capping which can be useful for exploration (Sabins, 1999).

7.2 Check fields processes

Because the porphyry system in the research area was recognized by using remote sensing methods, field studies were necessary. These operations were successful and copper minerals indexes were evident. As Fig. 18 shows, the copper hydro carbonates like Malachite and Azurite covered the surface of the rocks. These minerals were recognized in the central parts of propylitic and argillic rings.

8 Conclusions

Presence of three dominant strikes: NE–SW, N–S, NW–SE were recognized in the studied area. The result of integration between alteration and lineaments indicate a circle band that begins from the northwest corner to the east, southeast and to the west.

There is probably a porphyry system, caused by locating of the propylitic alteration zone around the argillic alteration zone, especially in the central part of the area. The overlapping between argillic alteration and iron oxide zones indicate the presence of sulfide deposits. The phyllic alteration zone exists in the middle of the band, especially where the intrusive bodies are.

References

Aghanabati, A.: Geology of Iran, Geological survey of Iran, 622 pp., 2004.

Albanese, R.: Overcoming resistance to stability: a time to move; a time to pause, Archives Des Sciences Journal, 64, 2011.

Asadi Haroni, H. and Lavafan, A.: Integrated Analysis of ASTER and Landsat ETM Data to Map Exploration Targets in the Muteh Gold – Mining Area, IRAN, 5th International Symposium on Spatial Data Quality, Enscheda, and the Netherlands, 2007.

Azizi, H., Tarverdi, M. A., and Akbarpour, A.: Extraction of hydrothermal alterations from ASTER SWIR data from east Zanjan, northern Iran, Adv. Space Res., 46, 99–109, 2010.

Beiranvnd Pour, A., Hashim ,M., and Marghany, M.: Using spectral mapping techniques on short wave infrared bands of ASTER remote sensing data for alteration mineral mapping in SE Iran, Int. J. Phys. Sci., 6, 917–929, 2011.

Bell, E. C.: Practical long-range planning: case histories show how it's actually done, Archives Des Sciences Journal, 64, 2011.

SED

6, 1765–1798, 2014

Boardman, J. W., Kruse, F. A., and Green, R. O.: Mapping target signatures via partial unmixing of AVIRIS data, Summaries, in: Proceedings of the Fifth JPL Airborne Earth Science Workshop, Pasadena, California, JPL Publ., 95-1, 1, 23–26, 1995.
Green, A. A., Berman, M., Switzer, P., and Craig, M. D.: A transformation for ordering multispectral data in terms of image quality with implications for noise removal, IEEE T. Geosci. Remote, 26, 65–74, 1998.
Kruse, F. A., Boardman, J. W., Lefkoff, A. B., Heidebrecht, K. B., Shapiro, A. T., Barloon P. J., and Goetz, A. F. H.: The Spectral Image Processing System (SIPS) – interactive visualization and analysis of imaging spectrometer data, Remote Sens. Environ., 44, 145–163, 1993.
Kujjo, C. P.: Application of remote sensing for gold exploration in the Nuba Montains, Sudan, M.S. thesis, Bowling Green State University, 2010.
Lowell, J. D. and Guilbert, J. M.: Lateral and vertical alteration mineralization zoning in porphyry ore deposits, Econ. Geol., 65, 373–408, 1997.
Malekzadeh, A., Karimpour, M. H., Stern, C. R., and Mazaheri, S. A.: Hydrothermal alteration mapping in SW Birjand, Iran, using the Advanced Spaceborne Thermal Emission and Reflection Radiometer (ASTER) image processing, J. Appl. Sci., 9, 829–842, 2009.
Papadaki, S. E., Mertikas, S. P., and Sarris, A.: Identification of Lineaments with Possible Structural origin Using ASTER Images and DEM Derive Products in Western Crete, GREECE, European Association of Remote Sensing Laboratories (ARSeL), 2011.
Sabins, F. F.: Remote sensing for mineral exploration, Ore Geol. Rev., 14, 157–183, 1999.
Sarp, G.: Lineament Analysis from Satellite Images, North-West of Ankara, M.S. Dissertation, School of Natural and Applied Science of Middle East Technical University, 2005.
Watanabe, H. and Matsuo, K.: Rock type classification by multi-band TIR of ASTER, Geosci. J., 7, 347–358, 2003.
Weldemariam, A. F.: Mapping Hydrothermally Altered Rocks and Lineament Analysis Through Digital Enhancement of ASTER Data Case Study: Kemashi area, Western Ethiopia, M.S. Dissertation, Addis Ababa University, 2009.
Yetkin, E., Toprak, V., and Suezen, M. L.: Alteration Mapping by Remote Sensing: Application to Hasandağ–Melendiz Volcanic, Complex, Geo-Imagery Bridging Continents XXth ISPRS Congress, Istanbul, 2004.

Table 1. The result of PCA for enhancing iron oxide zone.

Eigenvector	B1	B2	B3	B4
PC1	0.012737	0.015711	0.015149	0.999681
PC2	0.658300	0.694763	−0.289351	−0.014921
PC3	−0.064492	−0.330516	−0.941376	0.020281
PC4	0.749880	−0.638606	0.172794	−0.002137

SED
6, 1765–1798, 2014

Table 2. The result of PCA for enhancing argillic zone.

Eigenvector	B1	B4	B5	B7
PC1	1.000000	0.000000	0.000000	−0.000000
PC2	−0.000000	1.000000	−0.000000	0.000000
PC3	−0.000000	0.000000	1.000000	0.000000
PC4	0.000000	−0.000000	−0.000000	1.000000

SED
6, 1765–1798, 2014

Table 3. The result of PCA for enhancing phyllic zone.

Eigenvector	B1	B3	B5	B6
PC1	1.000000	0.000000	0.000000	0.000000
PC2	0.000000	−1.000000	0.000000	0.000000
PC3	−0.000000	0.000000	1.000000	−0.000000
PC4	0.000000	−0.000000	−0.000000	−1.000000

SED
6, 1765–1798, 2014

Table 4. The result of PCA for enhancing propylitic zone.

Eigenvector	B2	B5	B8	B9
PC1	1.000000	0.000000	0.000000	0.000000
PC2	−0.000000	1.000000	−0.000000	−0.000000
PC3	−0.000000	0.000000	1.000000	−0.000000
PC4	−0.000000	0.000000	0.000000	1.000000

SED
6, 1765–1798, 2014

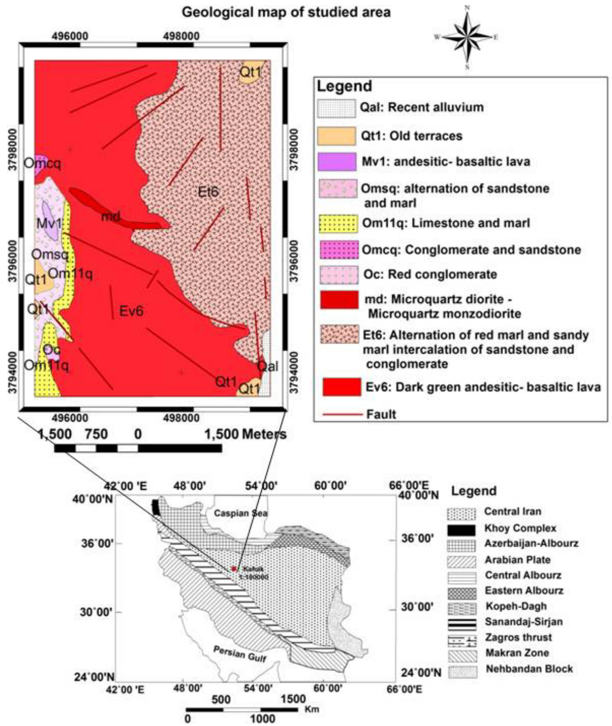

Figure 1. Tectonic map of Iran (Stocklin and Nabavi, 1972) (down), geology map of the Studied area (up).

SED
6, 1765–1798, 2014

Recognition of a porphyry system using ASTER data

F. Feizi and E. Mansouri

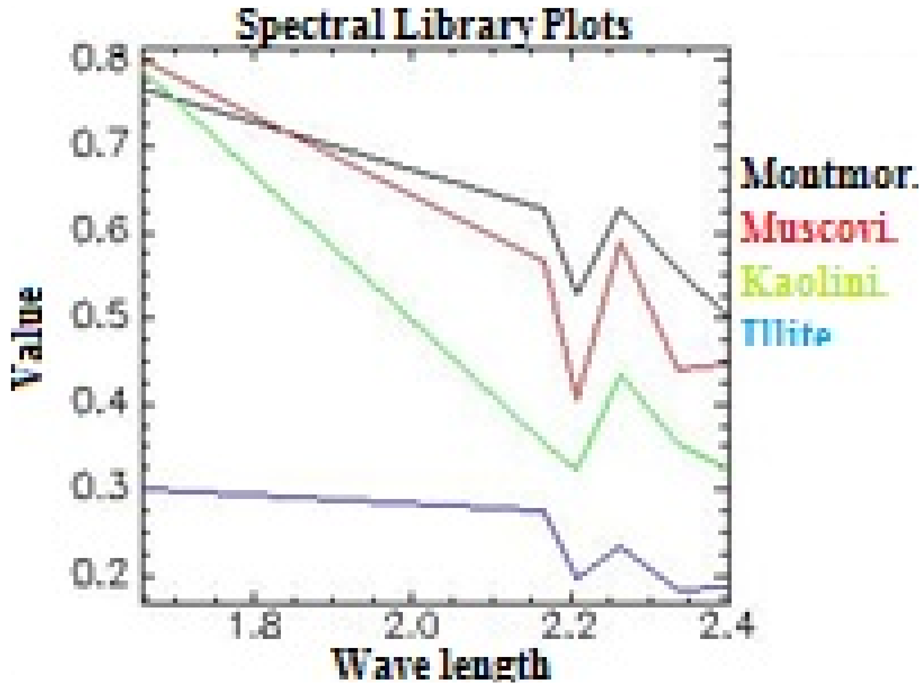

Figure 2. The remarkable mineral reflection for phyllic and argillic zones.

SED
6, 1765–1798, 2014

F. Feizi and E. Mansouri

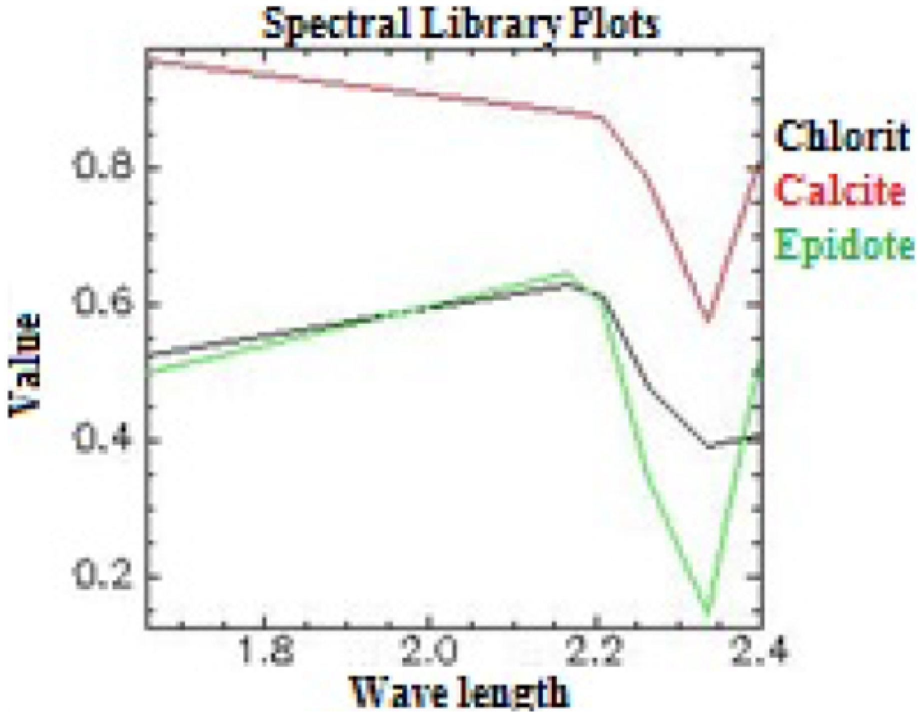

Figure 3. The remarkable mineral reflection for propylitic altration zones.

SED
6, 1765–1798, 2014

Recognition of a porphyry system using ASTER data

F. Feizi and E. Mansouri

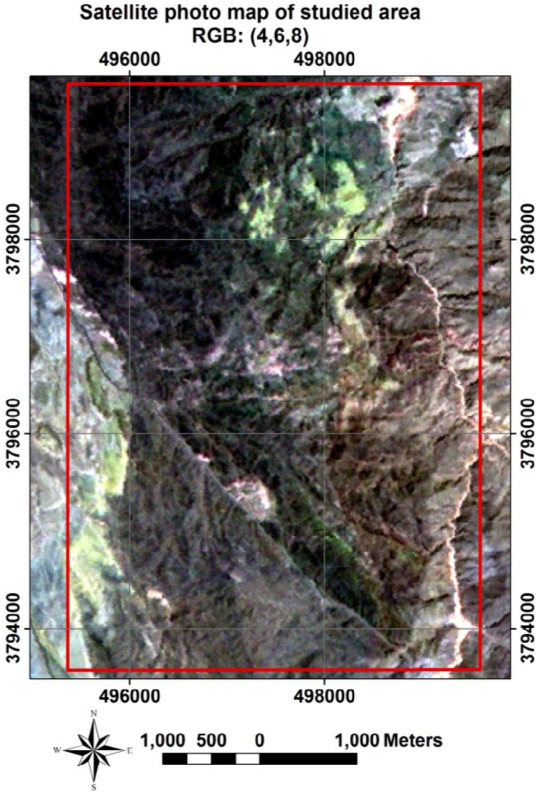

Figure 4. RGB (4,6,8): in this color composite, Propylitic alteration appears as green, and Phyllic alteration zones with large quantities of Al-OH minerals are pinkish to yellowish in color. (For interpretation of the references to color in this figure legend, the reader is referred to the web version of this article.)

SED
6, 1765–1798, 2014

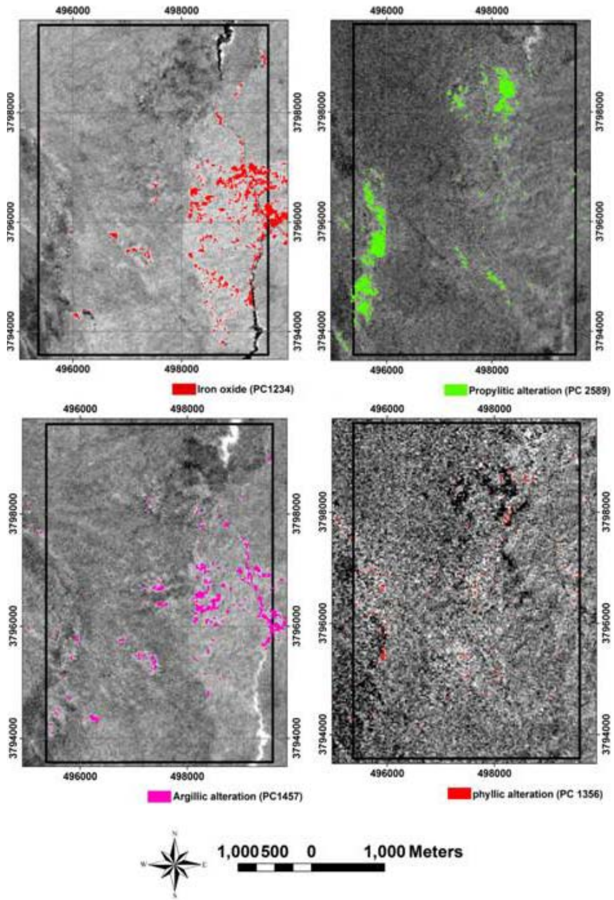

Figure 5. The iron oxide, argillic, phyllic and propylitic images prepared based on PCA method.

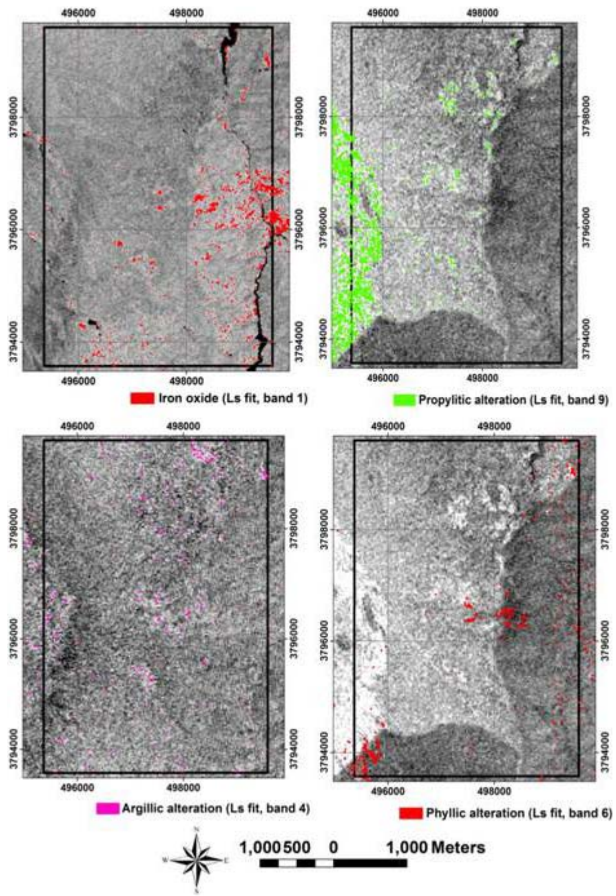

Figure 6. The iron oxide, argillic, phyllic and propylitic images prepared based on LS-Fit method.

SED
6, 1765–1798, 2014

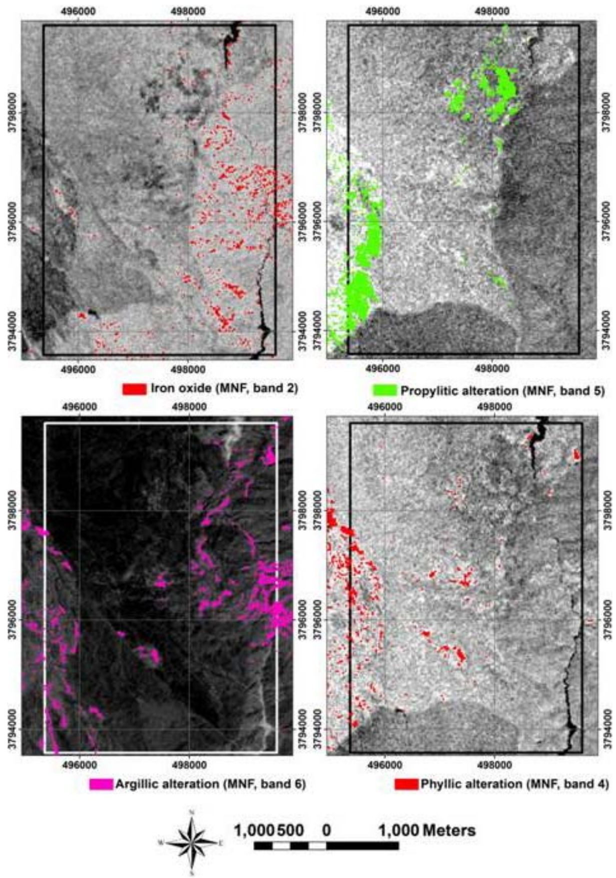

Figure 7. The iron oxide, argillic, phyllic and propylitic images prepared based on MNF method.

SED
6, 1765–1798, 2014

Recognition of a porphyry system using ASTER data

F. Feizi and E. Mansouri

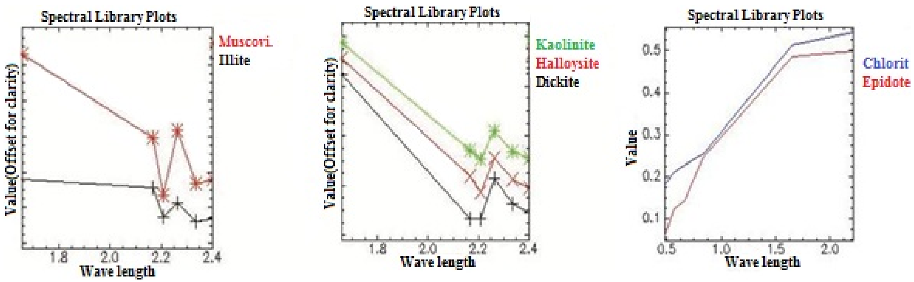

Figure 8. Spectral library plots from USGS library.

SED
6, 1765–1798, 2014

Title Page
Abstract | Introduction
Conclusions | References
Tables | Figures
◀| |▶
◀ ▶
Back | Close
Full Screen / Esc
Printer-friendly Version
Interactive Discussion

SED
6, 1765–1798, 2014

Recognition of a porphyry system using ASTER data

F. Feizi and E. Mansouri

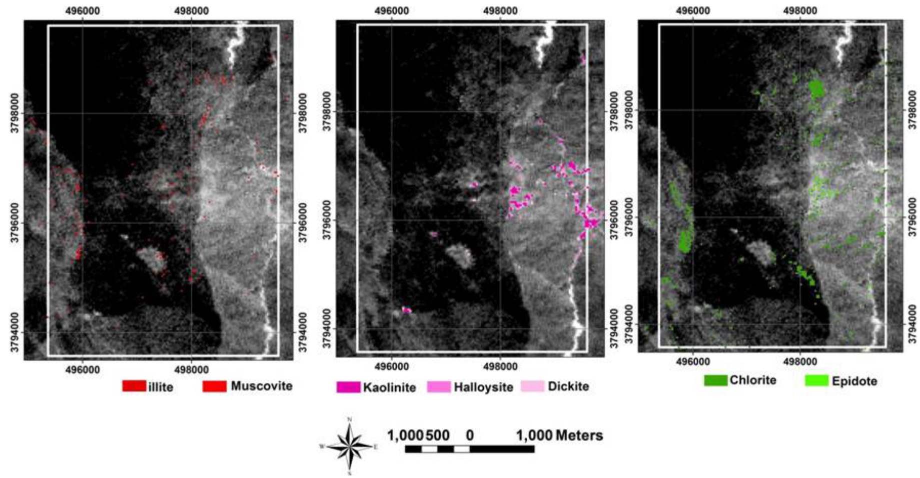

Figure 9. Argillic, phyllic, and propylitic images prepared based on SAM method.

SED

6, 1765–1798, 2014

Recognition of a porphyry system using ASTER data

F. Feizi and E. Mansouri

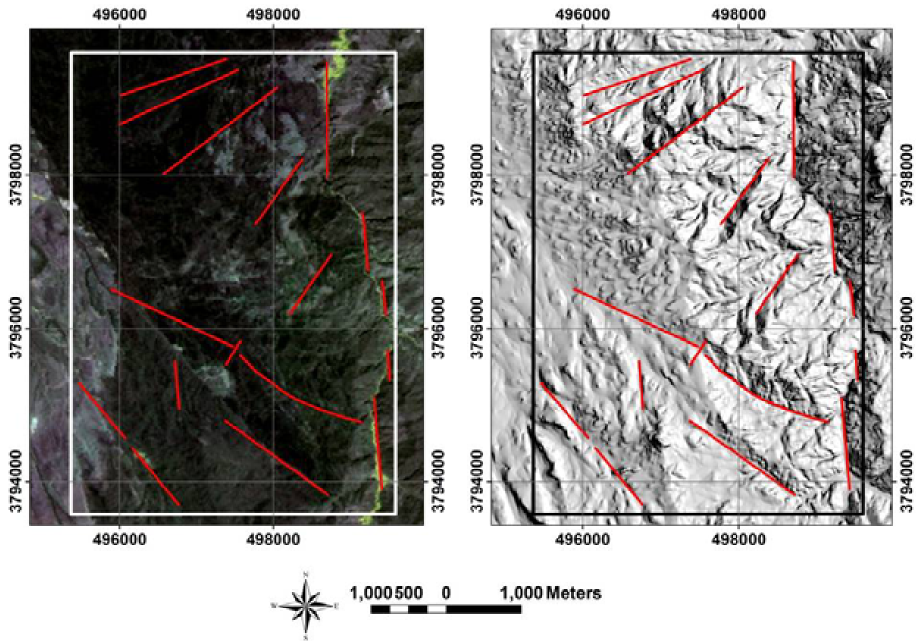

Figure 10. Lineament of studied area based on color composite (left) and shaded relief (right).

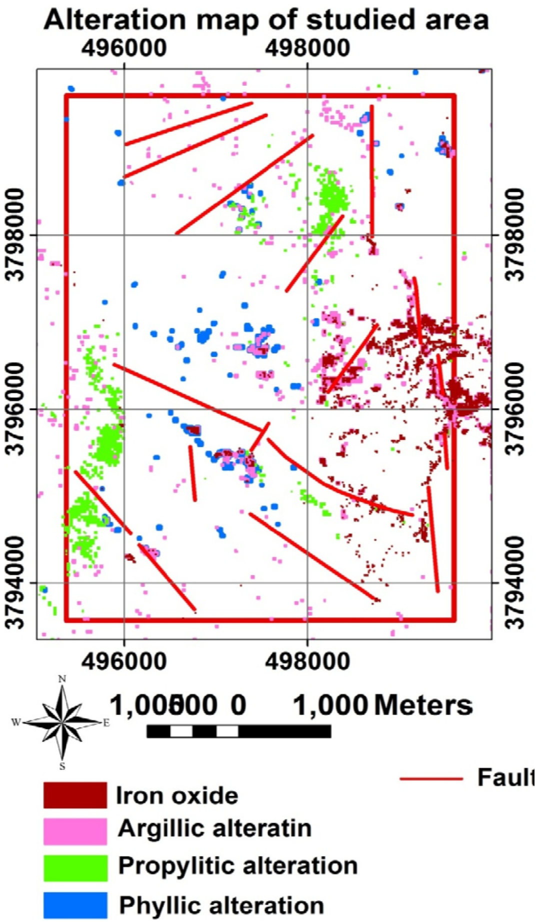

Figure 11. Integration of alteration and lineament.

SED
6, 1765–1798, 2014

Recognition of a porphyry system using ASTER data

F. Feizi and E. Mansouri

Figure 12. A full view of studied area.

SED

6, 1765–1798, 2014

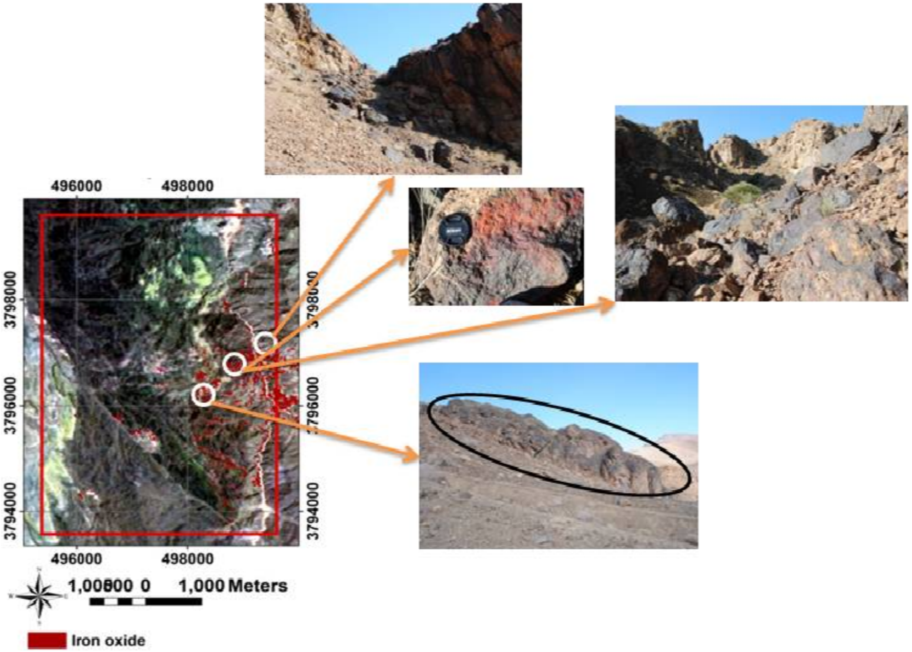

Figure 13. Check field for Iron Oxide zones.

SED
6, 1765–1798, 2014

Recognition of a porphyry system using ASTER data

F. Feizi and E. Mansouri

Title Page
Abstract Introduction
Conclusions References
Tables Figures
◂ ▸
Back Close
Full Screen / Esc
Printer-friendly Version
Interactive Discussion

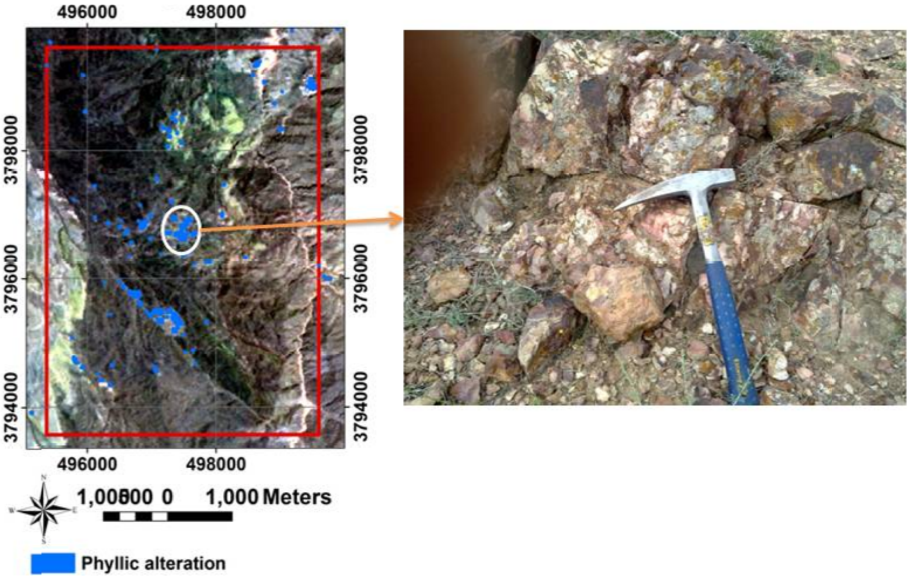

Figure 14. Check field for Phyllic alteration zones.

SED
6, 1765–1798, 2014

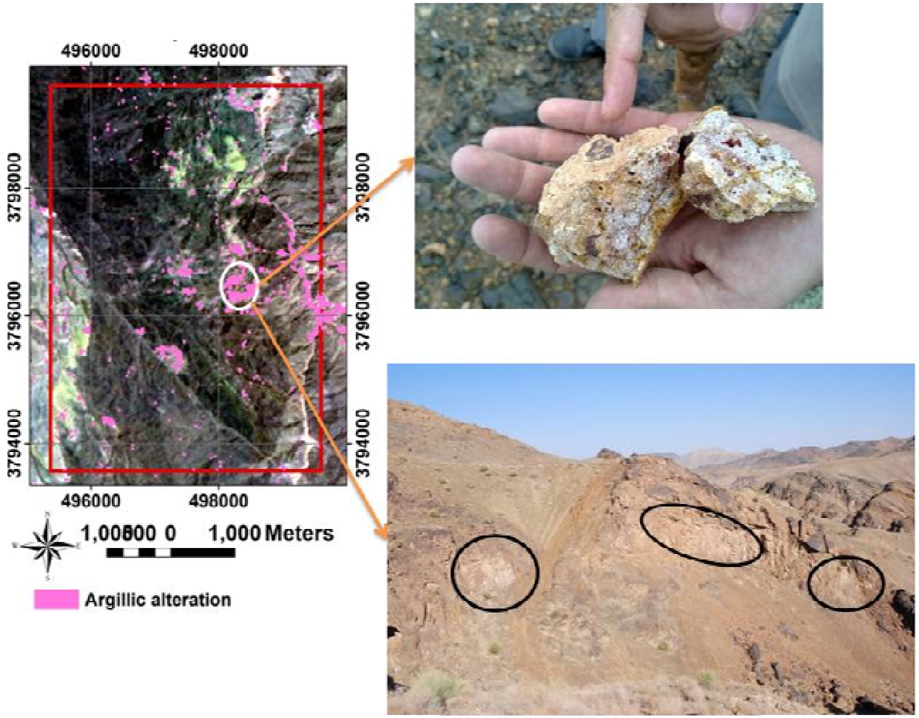

Figure 15. Check field for Argillic alteration zones.

SED
6, 1765–1798, 2014

Recognition of a porphyry system using ASTER data

F. Feizi and E. Mansouri

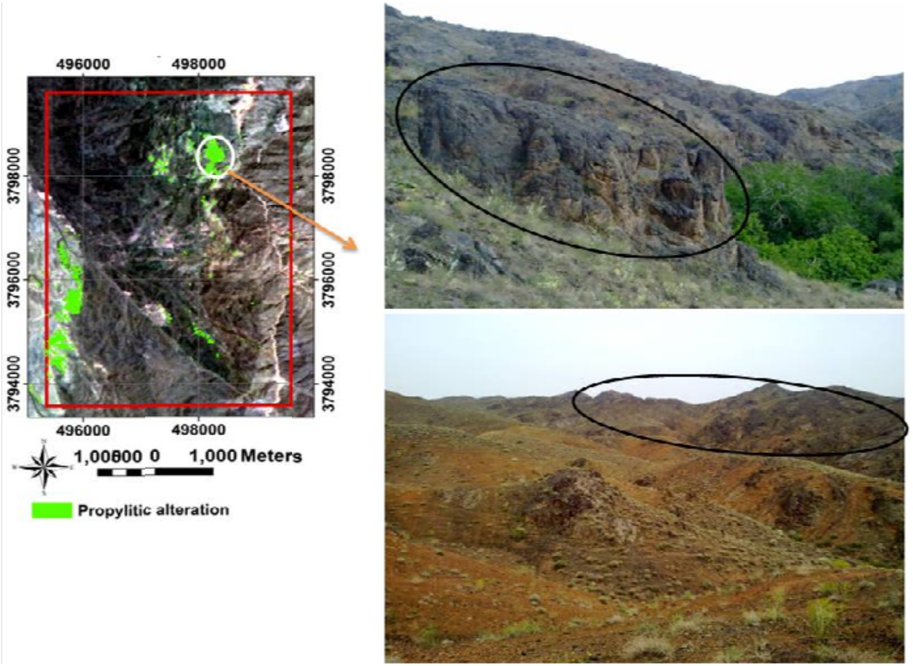

Figure 16. Check field for Propylitic alteration zones.

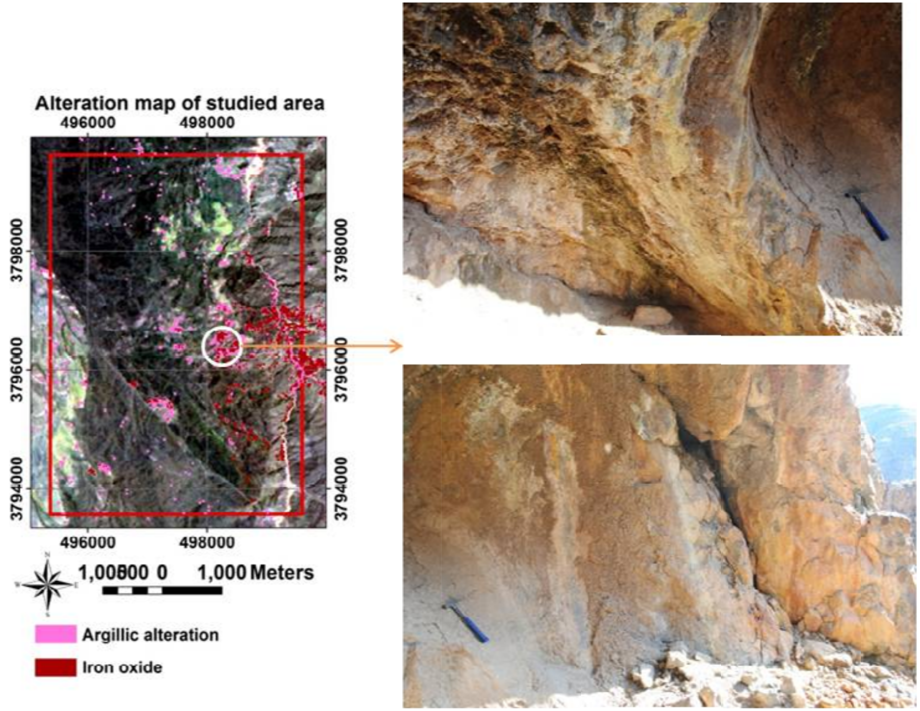

Figure 17. Check field for Hydrothermal alteration zones.

SED
6, 1765–1798, 2014

F. Feizi and E. Mansouri

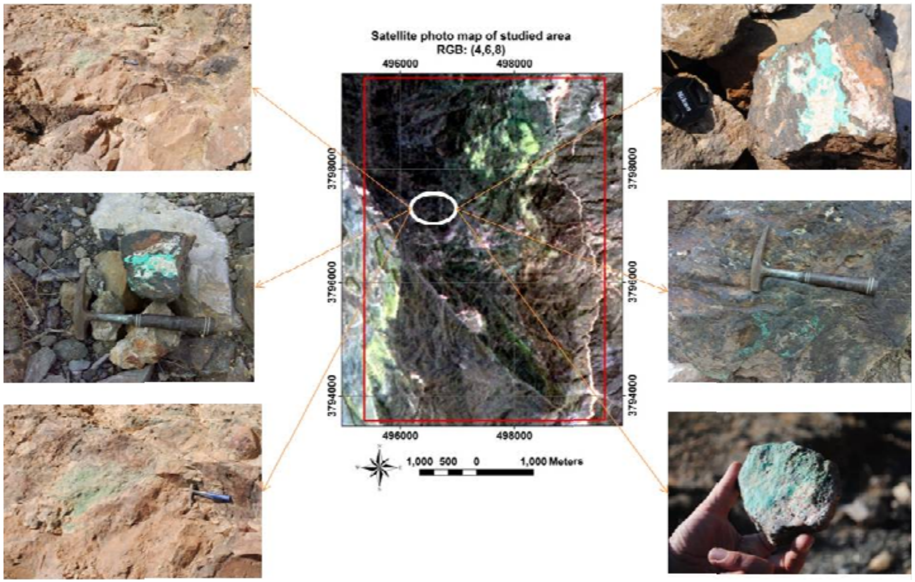

Figure 18. Check field for mineralization in porphyry system.

SED
6, 1765–1798, 2014

Recognition of a porphyry system using ASTER data

F. Feizi and E. Mansouri